ANNALS of Clinical and Translational Neurology
Open Access

RESEARCH ARTICLE

Dynamic causal modeling of reorganization of memory and language networks in temporal lobe epilepsy

Alireza Fallahi[1,2], Narges Hoseini-Tabatabaei[3], Fatemeh Eivazi[4,5,6], Neda Mohammadi Mobarakeh[4,6], Hamed Dehghani-Siahaki[4,6], Laila Alibiglou[7], Reza Rostami[8], Jafar Mehvari Habibabadi[9], Seyed-Sohrab Hashemi-Fesharaki[10], Mohammad Taghi Joghataei[7] & Mohammad-Reza Nazem-Zadeh[4,6,11]

[1]Control and Intelligent Processing Center of Excellence (CIPCE), School of Electrical and Computer Engineering, College of Engineering, University of Tehran, Tehran, Iran
[2]Biomedical Engineering Department, Hamedan University of Technology, Hamedan, Iran
[3]Medical School, Tehran University of Medical Sciences, Tehran, Iran
[4]Research Center for Molecular and Cellular Imaging, Advanced Medical Technologies and Equipment Institute (AMTEI), Tehran University of Medical Sciences, Tehran, Iran
[5]Institute for Cognitive and Brain Sciences, Shahid Beheshti University, Tehran, Iran
[6]Medical Physics and Biomedical Engineering Department, Tehran University of Medical Sciences, Tehran, Iran
[7]Department of Neuroscience, Iran University of Medical Sciences, Tehran, Iran
[8]Department of Psychology, University of Tehran, Tehran, Iran
[9]Isfahan Neuroscience Research Center, Isfahan University of Medical Sciences, Isfahan, Iran
[10]Pars Advanced Medical Research Center, Pars Hospital, Tehran, Iran
[11]Department of Neuroscience, Monash University, Melbourne, VIC, Australia

Correspondence
Mohammad-Reza Nazem-Zadeh, Advanced Medical Technologies and Equipment Institute (AMTEI), Tehran University of Medical Sciences, Tehran, Iran. Tel: + 98 21 66581505; Fax: + 98 21 66438630; E-mail: mnazemzadeh@tums.ac.ir, mohamad.nazem-zadeh@monash.edu

Received: 11 January 2023; Revised: 22 August 2023; Accepted: 10 September 2023

***Annals of Clinical and Translational Neurology* 2023; 10(12): 2238–2254**

doi: 10.1002/acn3.51908

Abstract

Objective: To evaluate the alterations of language and memory functions using dynamic causal modeling, in order to identify the epileptogenic hemisphere in temporal lobe epilepsy (TLE). **Methods:** Twenty-two patients with left TLE and 13 patients with right TLE underwent functional magnetic resonance imaging (fMRI) during four memory and four language mapping tasks. Dynamic causal modeling (DCM) was employed on fMRI data to examine effective directional connectivity in memory and language networks and the alterations in people with TLE compared to healthy individuals. **Results:** DCM analysis suggested that TLE can influence the memory network more widely compared to the language network. For memory mapping, it demonstrated overall hyperconnectivity from the left hemisphere to the other cranial regions in the picture encoding, and from the right hemisphere to the other cranial regions in the word encoding tasks. On the contrary, overall hypoconnectivity was seen from the brain hemisphere contralateral to the seizure onset in the retrieval tasks. DCM analysis further manifested hypoconnectivity between the brain's hemispheres in the language network in patients with TLE compared to controls. The CANTAB® neuropsychological test revealed a negative correlation for the left TLE and a positive correlation for the right TLE cohorts for the connections extracted by DCM that were significantly different between the left and right TLE cohorts. **Interpretation:** In this study, dynamic causal modeling evidenced the reorganization of language and memory networks in TLE that can be used for a better understanding of the effects of TLE on the brain's cognitive functions.

Introduction

Temporal lobe epilepsy (TLE) is the most common type of refractory focal epilepsy, for which resection surgery is an effective solution.[1] However, impairment of main cognitive functions such as memory and language is among the deleterious side effects of surgery in 30–40% of cases.

The language and memory networks are associated with temporal regions, and recurrent seizures can, therefore, change the function and structure of these networks. These changes are based on the phenomenon of neural flexibility that can occur in TLE patients over time.[2] Reorganization patterns can be more or less cognitively effective and cause varying degrees of language and memory impairment in patients with TLE[3–5] Therefore, preoperative assessments of potential postoperative effects can be crucial in the diagnosis of the patient's cognitive status in order to spare the candidate from the relatively high risk of cognitive decline arising from the surgery.

The functional competence of TLE structures and their impact on memory and language functions must be evaluated in cases involving unilateral temporal resections including hippocampectomy, amygdalohippocampectomy, and anterior temporal lobectomy. These structures include the hippocampus, and the Wernicke area, which is located in the posterior region of superior temporal gurus and involves language comprehension. Intracarotid sodium amobarbital procedure (ISAP) known as the "Wada test" measures the language and memory functions on one side of the brain at a time, determines their asymmetry (which brain's hemisphere controls the particular cognitive function), and how a prospective resection would interfere with the given function. However, ISAP is an invasive procedure that may cause transient or permanent damage and deficit and is not always accurate.

Functional MRI is a non-invasive neuroimaging technique that allows visualizing brain activity by measuring changes in blood oxygenation level-dependent (BOLD) in response to cognitive tasks. Cognitive imaging can be performed by recording fMRI data while the participant concurrently performs a cognitive task, during which specific brain areas are identified to be involved. It provides insights into how the brain processes information and implements cognitive functions including perception, attention, memory, decision-making, and language processing.[6] Given the essential role of clinical presentations in diagnostic procedures,[7,8] fMRI can be used to predict cognitive impairments and serves as a reliable method in preoperative evaluations.[9–11] It is an accurate preoperative diagnosis method with relatively high sensitivity and localizes and lateralizes anatomical regions and functional networks associated with language and memory. Task-based fMRI may help reduce the number of invasive diagnostic procedures required for accurate localization of seizure foci and the extent of damage caused to memory and language networks. Specifically, the advantage of fMRI compared with the ISAP test is its ability to localize language function more accurately in both cerebral hemispheres.

It can be hypothesized that while performing cognitive tasks in fMRI, the nodes within the cognitive networks involved during the task implementation in the brain demonstrate the causal influence on each other through effective functional connectivity. Effective connectivity can be measured by fMRI and dynamic causal modeling (DCM) as one of the most common methods for calculating and modeling the effective neural communication between brain regions and networks.[12,13] Several studies have examined the effect of TLE on the performance of memory and language networks using fMRI[14–16] including encoding and retrieval of abstract images, visual scenes, faces, words, object location, and spatial navigation tasks.[14,15,17–19] Several investigations have also used the DCM method to map the memory or language networks.[15,16,20]

Despite the promising results of these studies, fMRI activation analysis that examined the whole brain does not provide information about the connectivity of these regions. Based on previous research, the primary structures involved in episodic memory include the hippocampus, parahippocampus, entorhinal cortex, and perirhinal cortex, all of which are structures found in the temporal lobe of the cerebrum. It also includes the prefrontal cortex, precuneus, angular, and subcortical areas.[21,22] In addition, some structures in the mesial temporal lobe are more involved in memory encoding and some in retrieval phases. Visuospatial (nonverbal) memory is a cognitive process in everyday life and refers to the storage and transient manipulation of the visual information and spatial location of the object, followed by its retrieval.[23] The literature supports the mediation of mesial temporal structures (usually in the right hemisphere) in visuospatial memory.[24] Verbal memory, on the contrary, deals with the materials such as words and letters, that are primarily coded linguistically and maintained by a rehearsal process involving a subvocal sequential generation of memory items.[25] Language is conveyed over an extensive network of multiple functional areas to the frontal, temporal, and parietal lobes in both cerebral hemispheres. Broca's area and Wernicke's area have long been recognized as essential language centers. Further evidence has shown that other secondary and tertiary anatomical brain areas are also involved in language, including the supplementary motor area (SMA) and pre-SMA areas, dorsolateral prefrontal cortex, temporal pole, and middle and inferior temporal regions.[26–28] Several different word generation tasks are suitable to examine language networks, whereby language-associated memory, as well as other linguistic and cognitive processes, can also be assessed using task categories for the free generation of several words per trigger.[29] We, therefore, implemented different memory and language mapping protocols to study different aspects of such network-based reorganization by DCM. Based on this, four functional tasks were evaluated for each of the networks. Specifically, word encoding, picture encoding, word retrieval, and picture retrieval tasks were examined for memory mapping. In contrast, verbal fluency, semantics, passive listening, and word generation were evaluated for language mapping.

Previous fMRI/DCM research works have employed a limited number of brain regions within the memory and language networks to perform causal modeling and determine effective connectivity. Also, DCM studies are mainly using resting state fMRI data, which is not as sensitive and specific to special fMRI cognitive tasks. These certainly preclude a thorough evaluation of these networks and an understanding of the functional alterations as the mechanism of the implementation of these functions. Assuming all abovementioned nodes are maximally involved in the implementation of memory and language tasks (depending on the specific task to excite different regions among them with different weighted contributions), we implemented DCM to quantify the causal association of all nodes that are possibly involved in the implementation of memory and language tasks inside the brain and their functional alterations. We aimed to assess the reorganization of memory and language networks occurring due to TLE in terms of temporal and extratemporal directional connections. We evaluated the potential of dynamic causal modeling to extend our understanding of the mechanisms of alteration in memory and language networks in TLE patients and to identify biomarkers for lateralization of seizure onset.

Materials and Methods

Subject characteristics

This research was reviewed and approved by the Research Ethics Board (Institutional Review Board, IRB) of the Tehran University of Medical Sciences. Patients with severe cognitive impairment or other neurological diseases were excluded from the study. The patients with severe cognitive impairments at a level of preventing participation in the full structural, diffusion, or functional MRI study were also excluded. Thirty-five individuals with TLE (males: females, 16:19; left TLE: right TLE: 21:14; age range: 17–54 y; average age: 30.4 y) were recruited. Twenty-seven cases were identified with clear indications of mesial temporal sclerosis (MTS) (MR-positive), while eight cases did not have a clear sign of MTS based on MRI (MR-negative). Verbal intelligence quotient (VIQ) and performance intelligence quotient (PIQ) were also reported for TLE patients. Seventeen neurologically healthy control (HC) subjects (males: females, 8:9; age range: 20–42 years; average age: 28 years) were included (Table 1). All volunteers signed informed consent to participate in the study. Fourteen patients underwent surgical resection and achieved an Engel I outcome after 1 year, confirming the reliability of our criteria for establishing the epileptogenic side.

Image acquisition

All subjects were scanned using a 3-Tesla Siemens Magnetom Prisma MRI (Siemens Prisma, Erlangen, Germany) and a 64-channel phased-array head coil, with the software version of “Syngo MR E11” running at the machine.

Anatomic images were acquired using an inversion recovery MPRAGE (Magnetization Prepared—Rapid Gradient Echo Inversion Recovery) protocol. 3-D anatomical images were acquired for clinical diagnosis, including transverse T1-weighted images (TR = 1840 ms, TI = 900 ms, TE = 3.47 ms, flip angle = 8°, matrix = 256 × 256, slice thickness = 1.0 mm), in-plane resolution = 1.0 × 1.0 mm^2, pixel bandwidth = 250 Hz/pixel. T2-FLAIR images were also acquired using 3D-T2-SPACE (Sampling Perfection with Application optimized Contrasts using different flip angle Evolution) with imaging parameters of TR = 5000 ms, TI = 1800 ms, TE = 260 ms, flip angle = 120°–175°, voxel size = 1.0 × 1.0 × 1.0 mm, matrix = 256 × 256.

Functional MRI and gradient-echo planar images were acquired, providing blood oxygen level-dependent contrast with imaging parameters: Voxel size = 2.8 × 2.8 × 2.4 mm, Resolution—iPAT, PAT mode GRAPPA, Accel.

Table 1. Summary table of participant characteristics.

Characteristic	Left TLE	Right TLE	*P*-Value
Sample size	21	14	–
Sex (M/F)	10/11	8/6	0.73‡
Age (year), mean ± STD [range]	31.9 ± 8.2 [17–54]	26.8 ± 6.2 [17–36]	0.059*
Onset Age (years), mean ± STD [range]	10.8 ± 8.2 [0.5–29]	9.4 ± 9.4 [0.5–28]	0.6*
VIQ	97.6 ± 21 [60–139]	90.8 ± 23 [73–120]	0.22*
PIQ	93.3 ± 8.4 [79–115]	85.3 ± 9 [72 –105]	0.087*

Note that PIQ and VIQ were lower in RTLE compare to LTLE but not significantly different between the two groups (*P*-value = 0.22 for VIQ and *P*-value = 0.087 for PIQ). This could be due to the limited sample size.

PIQ, performance intelligence quotient; VIQ, verbal intelligence quotient.

‡Fisher's exact test.

*Two-sample *t*-test.

factor PE = 2, Ref. lines PE = 24, SNR = 1.00, Slices = 53, Dist. factor = 0%, Phase enc. dir. A ≫ P, FoV read = 220 mm, FoV phase = 100.0%, Base resolution = 80, Phase resolution 100%, Slice thickness = 2.4 mm, TR = 3000 ms, TE = 30.0 ms, Averages = 1, Filter Prescan Normalize, Fat sat., Reconstruction Magnitude, number of measurements = 140, Phase partial Fourier Off, Interpolation Off, Prescan Normalize On.

Task fMRI protocols

For memory mapping, four tasks were performed, including word encoding, picture encoding, word retrieval, and picture retrieval. Visual (nonverbal, pictures) and verbal (words) stimuli were visually presented during a single scanning session.[30] The fMRI paradigm consisted of alternating blocks of words as verbal stimuli and pictures as visual stimuli, with each of the 14 blocks. Each word block consisted of six words with a length between two and eight characters presented on screen for 18 s, followed by 12 s of a blank screen. In each word block, all words were either abstract or concrete, which took random turns in the next block. Each picture block consists of six pictures being presented on screen again for 18 s, followed by 12 s of a blank screen (Fig. 1). In each picture block, all pictures were either general scenes or nameable objects, which took a turn in the next block. To keep the participants engaged with full attention, they were instructed to indicate with a button press if they liked a word or picture. They were also asked to memorize the words for a delayed retrieval task following the encoding, where the memory was evaluated with a "seen"/"unseen" question. The 70 words/pictures presented during the encoding task were presented again intermixed with 42 new words/pictures as foils.

For language mapping, four tasks were performed, including visual-verbal fluency, semantic visual, passive listening, and word generation. The fMRI paradigm consisted of alternating blocks. For semantic visual, 14 blocks preceded, each presented on screen for 24 s, followed by 24 s on a blank screen. For verbal fluency, passive listening, and word generation, 5, 4, and 4 blocks preceded, respectively, each block presented on screen for the 30 s, followed by 30 s on a blank screen.

Preprocessing of functional MRI data

After reconstruction of the raw functional data, the first four images (first rest block- 12 sec) of each run were discarded to allow stabilization of the BOLD signal. Slice timing correction was done for the remaining volumes. Rigid body motion correction was applied by realigning to the session's first functional image, followed by spatial smoothing using a 6 mm full-width half-maximum (FWHM) Gaussian kernel. Using the normalization parameters estimated by the T1 structural image, the realigned functional volumes (voxel size [3, 3, 3]) were spatially normalized to the Montreal Neurological Institute (MNI) space DPARSF 4.3 (http://rfmri.org/dpabi) running in Matlab (version R2018b; The MathWorks, Natick, MA, USA).

Region of interest selection and time series extraction

The structures evidenced to be involved in the episodic memory and language processing (see in the introduction) were used as the regions of interest (ROIs).[22,31,32] For memory processing, the hippocampus, parahippocampus, entorhinal cortex, perirhinal cortex, and prefrontal cortex[21,22]; and for language processing, the Broca's and Wernicke's areas, dorsolateral prefrontal cortex, temporal pole, and middle and inferior temporal regions[26–28] were considered.

Tables 2 and 3 show the ROIs that were used for memory and language network analysis, respectively. Figure 2 also shows these ROIs on the brain cortex.

Effective connectivity for task-fMRI analysis

Effective connectivity analysis was performed using the DCM toolbox implemented in SPM12 (http://www.fil.ion.ucl.ac.uk/spm/) running in Matlab (version R2021b; The MathWorks, Natick, MA, USA). To infer directionality and context-dependent modulations, DCM uses differential equations to model inter-regional interactions. It is a hypothesis-driven modeling method testing for the effect of a task on and between regions. The constructed models calibrate the neuronal activity into hemodynamic responses and estimate the parameters based on the observed fMRI signal. To apply the DCM method, a set of models is defined with regions and their intrinsic connections in the form of a matrix labeled DCM-A. This is followed by applying task effect modulations to connections (DCM-B) and regions (DCM-C). The Bayesian estimation provides estimated parameters for each model and its subsequent connection and region as Ep.A, Ep.B, and Ep.C. In this study, only connection parameters (Ep. A) from the DCM were used to investigate connectivity patterns for controls and changes in connectivity as a function of TLE DCM uses a simple (deterministic) neural dynamics model in a network or graph of interacting brain regions.

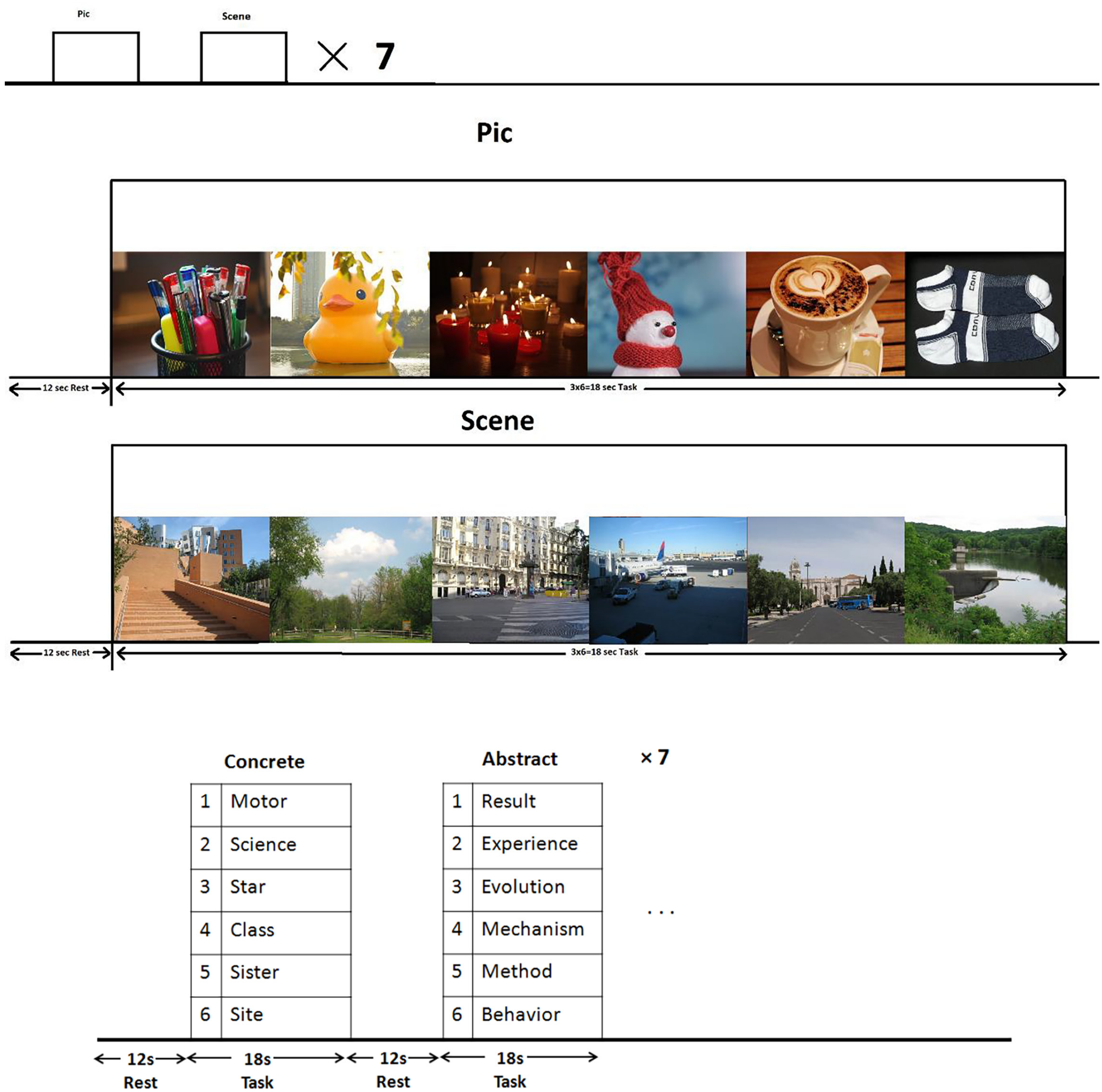

Figure 1. Sample task design for memory and language mapping.

Statistical analysis

The effective directional connectivity between L-TLE, R-TLE, and control groups was compared using a one-way ANOVA test. Then, each pair of groups was compared using a sample *t*-test. Left-TLE and right-TLE groups were compared using ANCOVA, controlling for the age covariate. The false discovery rate (FDR) algorithm was used to evaluate multiple comparisons at the 0.05 significance level.[33] For significant connections with FDR correction, the effect size was calculated using Cohen's d method.

Neuropsychological testing

All participants were assessed using standard cognitive tests by a trained clinical psychologist and covered executive functioning, including working memory, selective and sustained attention, visual recognition memory, manual reaction time, mental and motor speed, and social

Table 2. Region of interest for memory network.

Number	Brain region	Abbreviation	MNI coordinate
1	Left precuneus	L-P	−7, −56, 48
2	Right precuneus	R-P	10, −56, 44
3	Left hippocampus	L-HIP	−25, −20, −10
4	Right hippocampus	R-HIP	29, −20, −10
5	Left angular	L-ANG	−44, −60, 35
6	Right angular	R-ANG	45, −60, 38
7	Middle prefrontal cortex	MPFC	1, 55, −3
8	Left para hippocampus	L-PHIP	−21, −16, −20
9	Right para hippocampus	R-PHIP	25, −15, −20
10	Left perirhinal cortex	L-PRC	−19, −13, −34
11	Right perirhinal cortex	R-PRC	19, −13, −34
12	Left retrosplenial cortex	L-RSC	−14, −52, 8
13	Right retrosplenial cortex	R-RSC	14, −52, 8
14	Left entorhinal cortex	L-EC	−12, −2, −29
15	Right entorhinal cortex	R-EC	12, −2, −29
16	Left thalamus	L-THA	−11, −17, 8
17	Right thalamus	R-THA	13, −17, 8

Table 3. Regions of interest for language network.

Number	Brain region	Abbreviation	MNI coordinate
1	Left posterior middle temporal gyrus	L-PMTG	−56, −34, −2
2	Left inferior frontal gyrus, pars triangularis	L-IFG_PT	−50, 28, −2
3	Left middle temporal gyrus	L-MTG	−62, −44, 6
4	Left posterior supramarginal gyrus	L-PSG	−60, −50, 10
5	Left inferior frontal gyrus, pars opercularis	L-IFG_PO	−54, 18, 18
6	Left temporal pole	L-TP	−54, 6, −18
7	Superior frontal gyrus	S-FG_1	−4, 16, 62
8	Superior frontal gyrus	S-FG_2	−6, 30, 58
9	Right posterior superior temporal gyrus	R-PSTG	52, −36, 2
10	Frontal pole	FP	−8, 48, 42
11	Left middle frontal gyrus	L-MFG	−42, 4, 56
12	Right temporal pole	R-TP	52, 12, −18

cognition. The digital cognitive tests were administered with Cambridge Neuropsychological Test Automated Battery (CANTAB®; Cambridge Cognition) software. The Paired Associates Learning (PAL; CANTAB®) task, a test for assessing visual memory and new learning, and the Pattern Recognition Memory (PRM; CANTAB®) task, an examination of visual pattern recognition in a two-choice forced discrimination paradigm, were used to probe memory performance. Twelve cognitive test scores (7 PAL and 5 PRM tests) were obtained. Seven PAL tests include Total trials, Total errors, Stages completed on the first trial, Mean trials to success, Mean errors to success, and First trial memory score. Five PRM tests include Mean correct latency, Number correct, Percent correct, and Number incorrect.

Results

Memory mapping DCM results

Using the picture retrieval task, patients with left-TLE compared with the control group (Bonferroni corrected $P < 0.05$) showed hyperconnectivity from L-ANG to L-THA, R-RSC, and L-RSC and also hypoconnectivity from L-PHIP to L-P, L-EC to L-P, and R-P and also L-RSC to MPFC. Patients with right-TLE compared with the control group (Bonferroni corrected $P < 0.05$) showed hyperconnectivity from L-ANG to L-RSC, L-THA, and R-RSC and from MPFC to R-PRC and also hypoconnectivity from R-PHIP to L-P and R-P and R-HIP to L-THA. Comparing Left-TLE with Right-TLE groups (Bonferroni corrected $P < 0.05$) indicated hypoconnectivity from L-RSC to R-PRC, L-HIP to R-HIP, and from L-PHIP to R-EC (Fig. 3).

Using the picture encoding task, patients with left-TLE compared with the control group (Bonferroni corrected $P < 0.05$) show hyperconnectivity from L-HIP to L-P, R-P and R-ANG, L-RSC to L-ANG and R-ANG, R-PRC to L-PHIP, and also hypoconnectivity from MPFC to L-RSC and L-EC to R-ANG. Comparing right-TLE with the control group (Bonferroni corrected $P < 0.05$) shows hyperconnectivity from L-HIP to L-RSC and R-ANG, L-PHIP to R-PRC and L-RSC to R-ANG, and also hypoconnectivity from L-P and L-EC to R-ANG. Comparing left-TLE with right-TLE groups (Bonferroni corrected $P < 0.05$) shows only hypoconnectivity from L-PHIP to R-EC (Fig. 3).

Using the word encoding task, patients with left-TLE compared with the control group (Bonferroni corrected $P < 0.05$) show hyperconnectivity from L-HIP to R-PRC, R-EC to L-PRC, L-PRC, and R-PRC to LRSC and hypoconnectivity from R-ANG to P-RPC and vice versa and from R-THA to R-EC. Comparing right-TLE with the control group (Bonferroni corrected $P < 0.05$) shows hyperconnectivity from R-PRC to R-RSC and L-RSC, L-HIP to R-PHIP, and R-RSC to L-ANG, and also hypoconnectivity from RRSC and L-RSC to L-PRC, L-ANG to R-PRC. Comparing the left-TLE with a right-TLE group (Bonferroni corrected $P < 0.05$) shows hyperconnectivity from R-ANG to L-PRC and hypoconnectivity from L-RSC to R-EC and L-HIP (Fig. 4).

Using the word retrieval task, there is no significant difference between patients with left-TLE compared to the control group. Patients with right-TLE compared to the control group (Bonferroni corrected $P < 0.05$) show

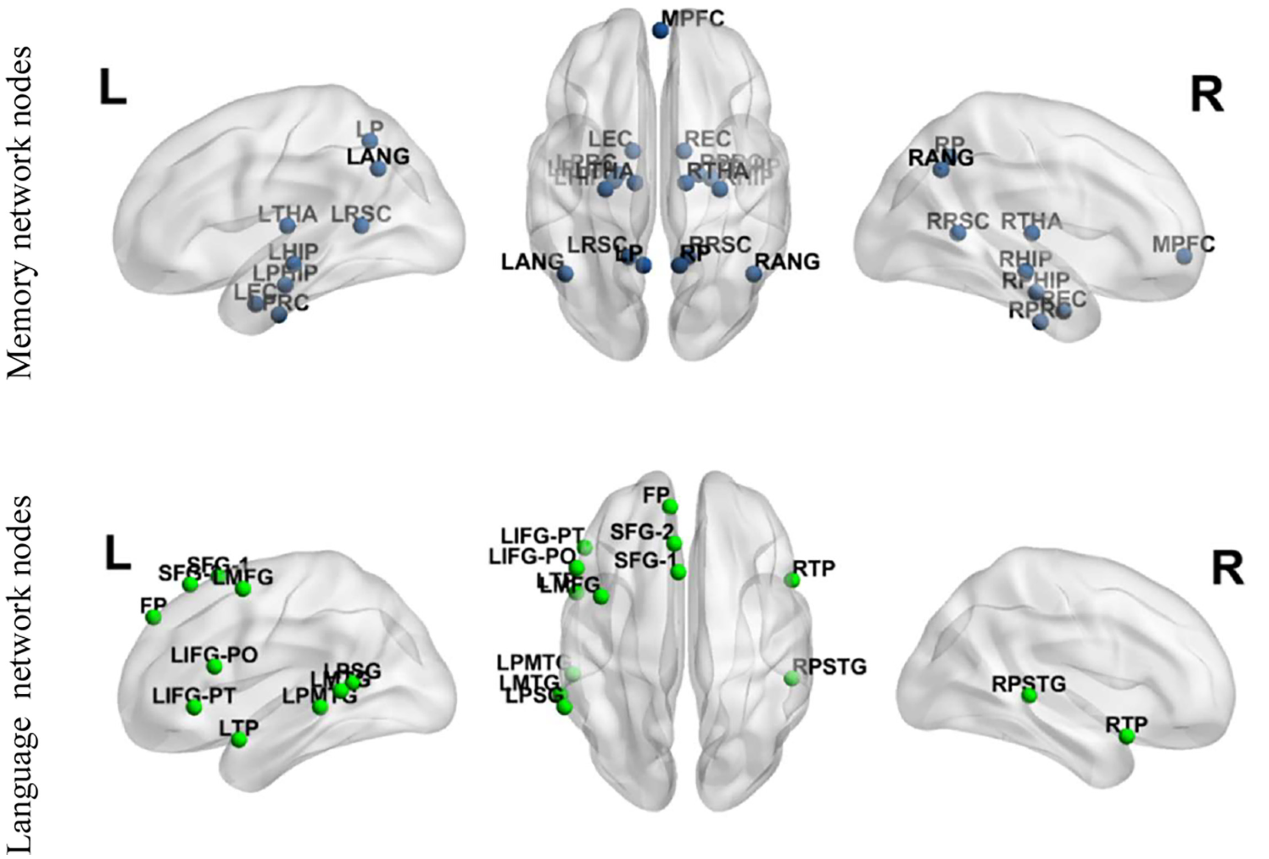

Figure 2. Memory and language network nodes. FP, Frontal pole; L-ANG, left angular; L-EC, left EC; L-HIP, left hippocampus; L-IFG_PO, left inferior frontal gyrus, pars opercularis; L-IFG_PT, left inferior frontal gyrus, pars triangularis; L-MFG, left middle frontal gyrus; L-MTG, left middle temporal gyrus; L-PHIP, left Para Hippocampus; L-PMTG, left posterior middle temporal gyrus; L-PRC, left PRC; L-PSG, left posterior supramarginal gyrus; L-RSC, left RSC; L-THA, left thalamus; L-TP, left temporal pole; MPFC, middle PFC; R-ANG, right angular; R-EC, right EC; R-HIP, right hippocampus; R-PHIP, right para hippocampus; R-PRC, right PRC; R-PSTG, right posterior superior temporal gyrus; R-RSC, right RSC; R-THA, right thalamus; R-TP, right temporal pole; SFG_1, superior frontal gyrus; SFG_2, superior frontal gyrus.

hyperconnectivity from L-PRC to R-EC and hypoconnectivity MPFC to L-RSC and R-RSC. Comparing the left-TLE with a right-TLE group (Bonferroni corrected $P < 0.05$) shows hyperconnectivity from L-THA to L-PRC and REC (Fig. 4).

All effect sizes were larger than 1, considered as large. For the significant connections between Left-TLE and Right-TLE groups, we represented bar plots for each connection in each Left-TLE, Right-TLE, and HC group in Figure 5.

Language mapping DCM results

Using a passive listening task, patients with left-TLE compared with the control group (Bonferroni corrected $P < 0.05$) show hyperconnectivity from L-MFG to SFG_2 and hypoconnectivity from L-PMTG to R-PSTG, L-IFG_PT to L-TP, L-IFG_PO to L-TP and R-TP to L-PMTG. Patients with right-TLE compared with the control group (Bonferroni corrected $P < 0.05$) show hyperconnectivity from L-MTG to FP and hypoconnectivity from L-PSG to R-TP, L-PSG to L-MTG, and R-TP to L-PSG. There is no significant difference between the left-TLE and right-TLE groups (Bonferroni corrected $P < 0.05$) (Fig. 6). Since the MNI coordinate for the left posterior superior temporal gyrus (-56 -34 -2) is very close to the MNI coordinate for the L-PMTG (left posterior middle temporal gyrus) (52–36 2), an ROI sphere with the radius of 8 mm will merge it into the L-PMTG, that actually contains "left posterior superior temporal gyrus".

Using semantic task, patients with left-TLE compared with the control group (Bonferroni corrected $P < 0.05$) show hyperconnectivity from R-TP to FP and hypoconnectivity from L-MTG and L-PSG to R-TP. Patients with right-TLE compared with the control group (Bonferroni

Task	Left-TLE vs. Control	Right-TLE vs. Control	Left-TLE vs. Right TLE
Picture Encoding	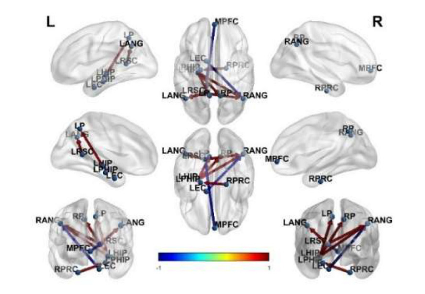	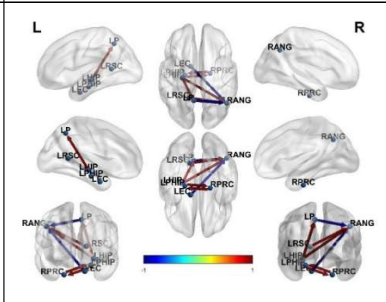	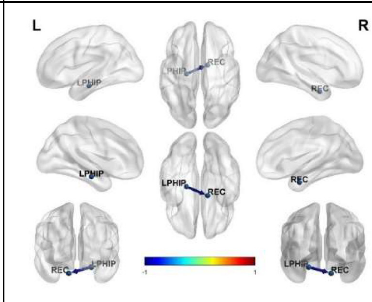
	L-HIP → L-P (2) L-HIP →R-P (1.65) L-HIP →R-ANG (1.74) L-RSC → L-ANG (1.87) L-RSC →R-ANG (1.89) R-PRC → L-PHIP (1.87) MPFC → L-RSC (2.26) L-EC → R-ANG (1.43)	L-HIP → LP (2.1) L-HIP → R-ANG (1.8) L-PHIP → R-PRC (1.88) L-RSC → R-ANG (1.36) L-P → R-ANG (1.63) L-EC → R-ANG (1.7)	R-HIP → R-HIP (1.5) L-PHIP → R-EC (1.47) R-RSC → R-RSC (1.35)
Picture Retrieval	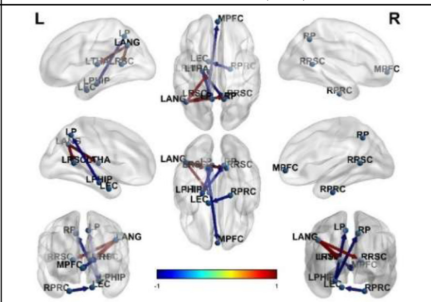	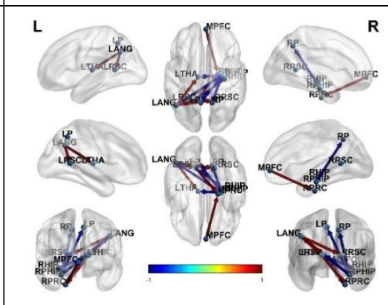	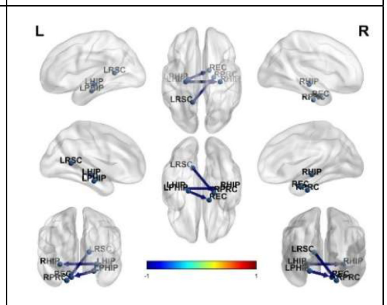
	L-ANG → L-THA(1.7) L-ANG → L-RSC (1.59) L-ANG → R-RSC (1.57) L-PHIP → L-P (1.6) L-PHIP → R-P (1.6) RPRC → L-EC (1.5) L-RSC → MPFC (2)	L-ANG → L-THA (1.4) L-ANG → L-RSC (1.1) L-ANG → R-RSC (1.4) MPFC → R-PRC (1.7) R-PHIP → L-P (1.4) R-PHIP → R-P (1.8) R-PHIP → L-ANG (2.3) R-PHIP → L-THA (1.4) RHIP →LRSC (1.7)	L-RSC → R-PRC (1.2) L-HIP → R-HIP (1.1) L-PHIP → R-EC (1.4)
Red color: hyperconnectivity, Blue color: hypoconnectivity, (Effect size)			

Figure 3. Result of significant difference in effective connectivity between left-TLE, right-TLE, and control groups using memory mapping tasks in picture encoding and retrieval tasks. L-ANG, left angular; L-EC, left EC; L-HIP, left hippocampus; L-PHIP, left para hippocampus; L-PRC, left PRC; L-RSC, left RSC; L-THA, left thalamus; MPFC, middle PFC; R-ANG, RIGHT ANGULAR; R-EC, right EC; R-HIP, right hippocampus; R-PHIP, right para hippocampus; R-PRC, right PRC; R-RSC, right RSC; R-THA, right Thalamus.

corrected $P < 0.05$) show hypoconnectivity from LMTG to R-TP and vice versa. There is no significant difference between the left-TLE and right-TLE groups (Bonferroni corrected $P < 0.05$) (Fig. 6).

Using the verbal fluency task, patients with left-TLE compared with the control group (Bonferroni corrected $P < 0.05$) show hyperconnectivity from L-IFG_PO and L-IFG_PT to SFG_2. Patients with right-TLE compared with the control group (Bonferroni corrected $P < 0.05$) show hypoconnectivity from L-MTG to R-TP and vice versa. There is no significant difference between the left-TLE and right-TLE groups (Bonferroni corrected $P < 0.05$) (Fig. 6). Using the word generation task, there is no significant difference between any of the groups (Fig. 6).

All effect sizes were larger than 1 (considered a large effect size).

For more explanation about the FDR correction on significant connections on both memory and language connectivity results, the hypo- and hyperconnections and

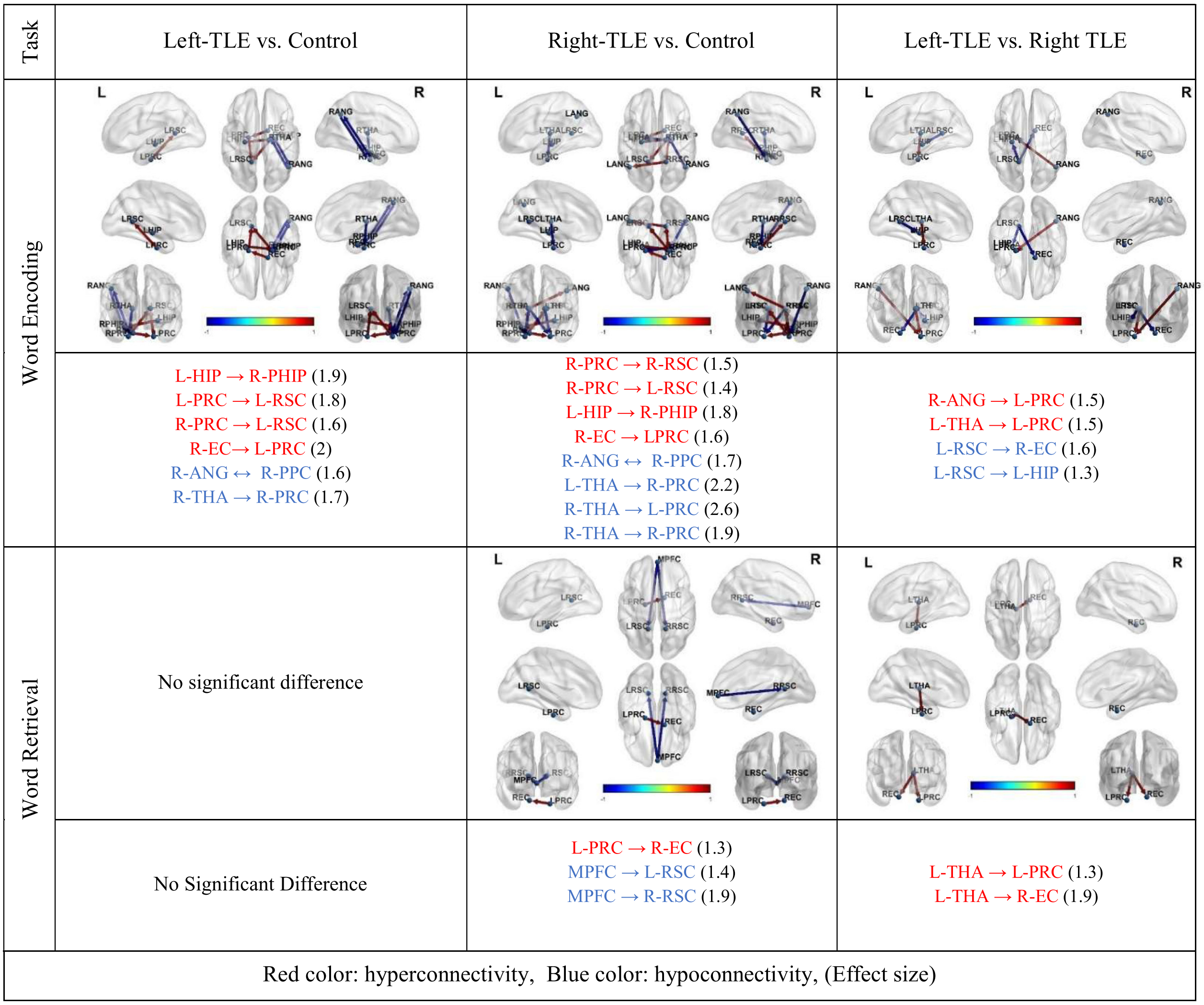

Figure 4. Result of significant difference in effective connectivity between left-TLE, right-TLE, and control groups using memory mapping tasks in word encoding and retrieval tasks. L-ANG, left angular; L-EC, left EC; L-HIP, left hippocampus; L-PHIP, left para hippocampus; L-PRC, left PRC; L-RSC, left RSC; L-THA, left thalamus; MPFC, middle PFC; R-ANG, right angular; R-EC, right EC; R-HIP, right hippocampus; R-PHIP, right para hippocampus; R-PRC, right PRC; R-RSC, right RSC; R-THA, right thalamus.

marking the ones that survived FDR and ones that did not survive mentioned in Tables S1 and S2 of the Supplementary materials.

CANTAB PAL and PRM

Figure 7 shows a box plot that compares the CANTAB tests between two left and right TLE groups. PAL Stages were completed on the first trial, and PRM Mean correct latency showed a significant difference ($P < 0.05$) between the two right and left TLE groups.

We performed a correlation analysis to examine the independent influence of each of the cognitive test variables on connectivity parameters. In both TLE groups, robust correlations between the value of directional connections and cognitive test performance were observed in some memory tasks. In the picture encoding task (Fig. 8), for the left TLE group the connection from R-HIP to R-HIP displayed a significant negative correlation with PAL total trial, PAL Mean trial to success, PAL Mean errors to success ($r = -0.65$, $P = 0.02$; $r = -0.66$, $P = 0.04$; $r = -0.56$, $P = 0.01$, respectively) and the connection from R-RSC to R-RSC displayed a significant negative correlation with PAL Mean errors to success ($r = -0.6$, $P = 0.02$). In the picture retrieval task (Fig. 8), in the left TLE group the connection from L-HIP to R-HIP

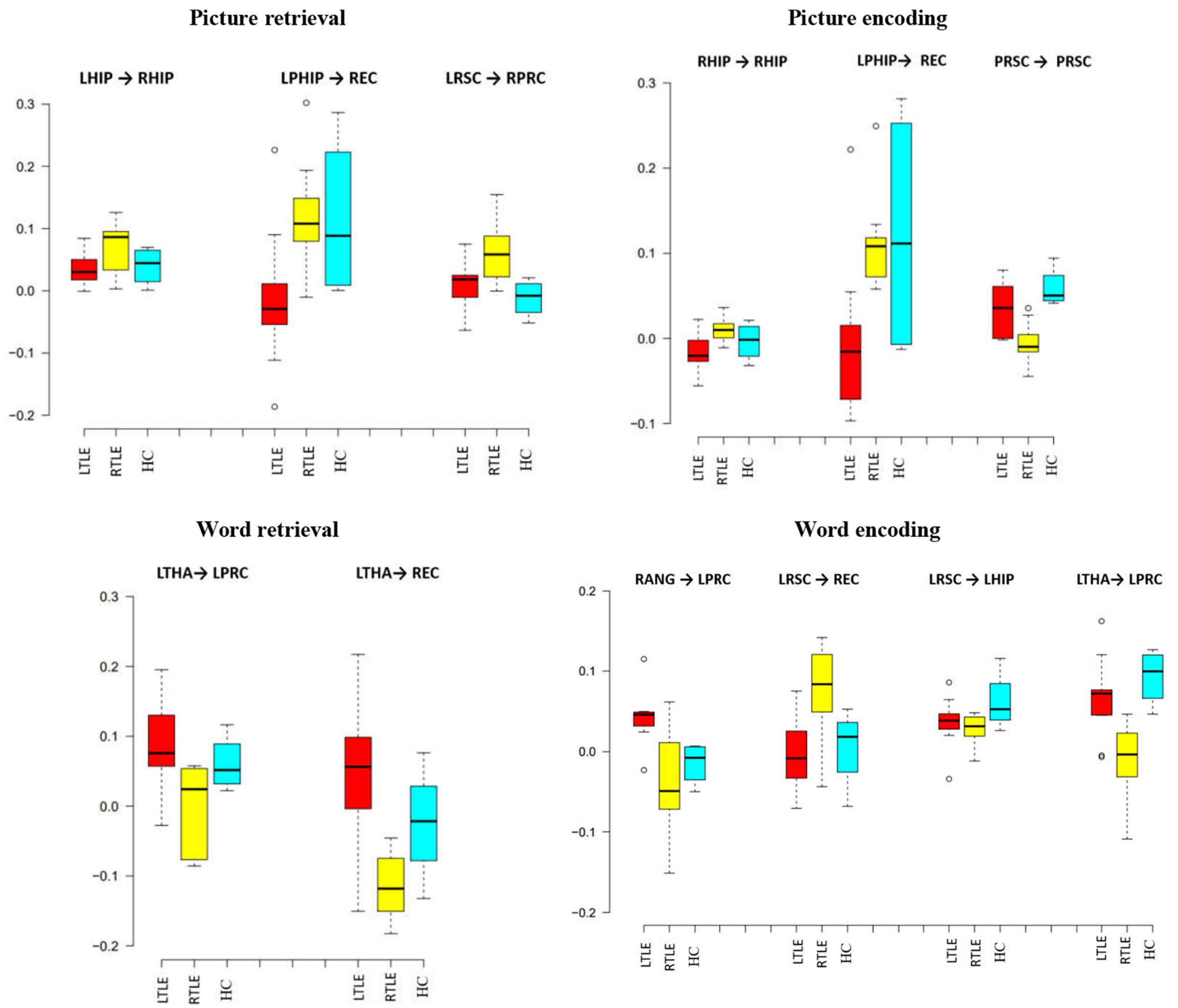

Figure 5. Bar graph for significant connection between Left-TLE and Right-TLE groups for memory mapping tasks. Red graphs represent the Left-TLE group, yellow graphs represent the Right-TLE group and blue graphs represent the HC group.

displayed a significant negative correlation with PAL total trial and PAL mean trial to success ($r = -0.53$, $P = 0.03$; $r = -0.45$, $P = 0.03$, respectively). Moreover, for the right TLE group the connection from L-HIP to R-HIP displayed a significant positive correlation with PAL total trial and PAL mean trial to success ($r = 0.43$, $P = 0.03$; $r = 0.43$, $P = 0.03$, respectively). Furthermore, for the same group, the connection from L-PHIP to R-EC displayed a significant positive correlation with PAL total trial, PAL total error, PAL mean trial to success, and PAL Mean errors to success ($r = 0.45$, $P = 0.03$; $r = 0.55$, $P = 0.03$; $r = 0.55$, $P = 0.01$; $r = 0.45$, $P = 0.03$, respectively).

In the word encoding task (Fig. 9), for the left TLE group the connection from R-RSC to L-ANG displayed a significant negative correlation with PAL total trial, PAL

Figure 6. Result of significant difference in effective connectivity between left-TLE, right-TLE, and control groups using language mapping task. FP, frontal pole; L-IFG_PO, left inferior frontal gyrus, pars opercularis; L-IFG_PT, left inferior frontal gyrus, pars triangularis; L-MFG, left middle frontal gyrus; L-MTG, left middle temporal gyrus; L-PMTG, left posterior middle temporal gyrus; L-PSG, left posterior supramarginal gyrus; L-TP, left temporal pole; R-PSTG, right posterior superior temporal gyrus; R-TP, right temporal pole; SFG_1, superior frontal gyrus; SFG_2, superior frontal gyrus.

Task	Left-TLE vs. Control	Right-TLE vs. Control	Left-TLE vs. Right TLE
Passive	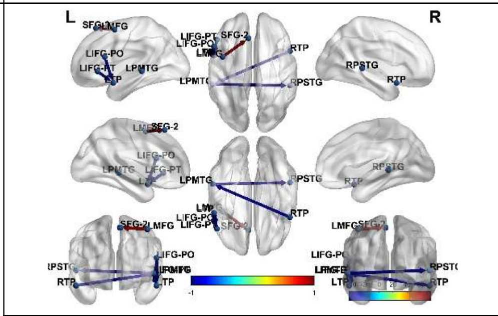	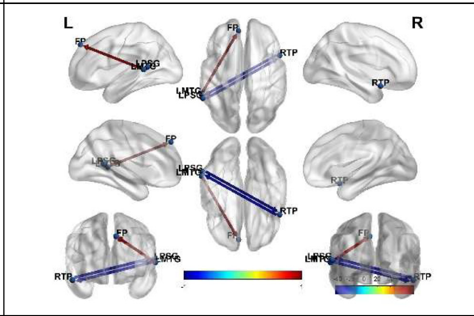	No Significant Difference
	L-MFG → SFG_2 (1.2) L-PMTG → R-PSTG (1) L-IFG_PT → L-TP (1.3) L-IFG_PO → L-TP (1.3) R-TP → L-PMTG (1.2)	L-MTG → FP (1.2) L-PSG → R-TP (1.2) L-PSG → L-MTG (1.2) R-TP → L-PSG (1.2)	
Semantic	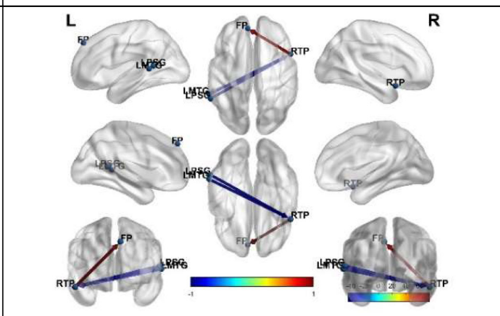	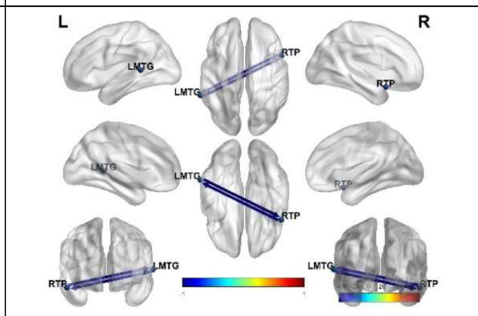	No Significant Difference
	R-TP → FP (1.3) L-MTG → R-TP (1.1) L-PSG → R-TP (1.4)	L-MTG ↔ R-TP (1.4)	
Verbal fluency	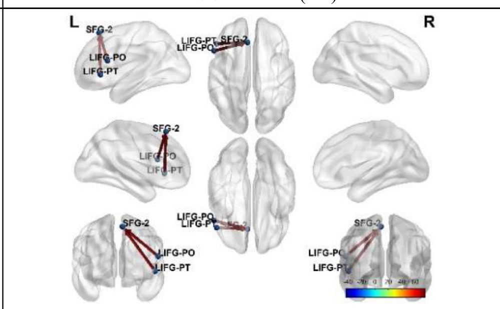	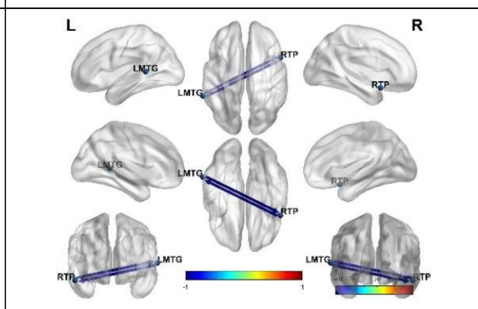	No Significant Difference
	L-IFG_PO → SFG_2 (1.1) L-IFG_PT → SFG_2 (1.1)	L-MTG ↔ R-TP (1.9)	
Word generation	No Significant Difference	No Significant Difference	No Significant Difference
Red color: hyperconnectivity, Blue color: hypoconnectivity, (Effect size)			

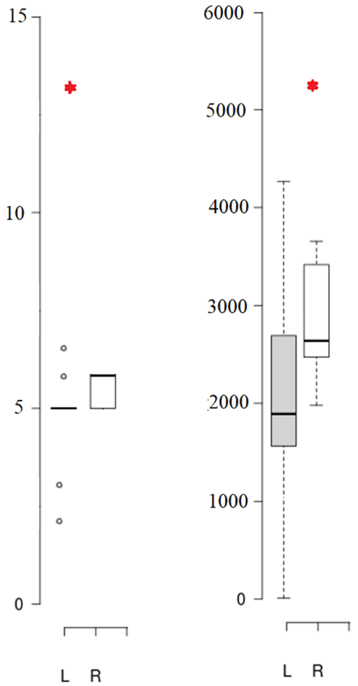

Figure 7. Box plot representation of CANTAB PAL and PRM tests with a significant difference between left and right TLE groups. The red stars denote significant differences between the two groups (*t*-test *P*-value < 0.05). L, left TLE group; PAL SCFT, PAL stages completed on the first trial; PRM MCL, PRM mean correct latency; R, right TLE group.

total error, PAL means trial to success, and PAL mean error to success ($r = -0.45$, $P = 0.004$; $r = -0.55$, $P = 0.03$; $r = -0.55$, $P = 0.001$; $r = -0.45$, $P = 0.03$, respectively), the connection from R-EC to L-PRC displayed a significant negative correlation with PRM percent correct ($r = -0.47$, $P = 0.001$) and the connection from R-PRC to L-RSC displayed a significant negative correlation with PAL mean trial to success ($r = -0.53$, $P = 0.03$). Finally, in the word retrieval task for the left TLE group, the connection from LTHA to REC significantly negatively correlated with the PAL total trial ($r = -0.53$, $P = 0.02$).

Discussion

In the present study, we investigated the functional properties of memory and language networks in TLE patients. To this end, we applied the DCM method to examine four memory tasks including encoding and retrieval of words and pictures, and four language tasks including passive listening, visual-verbal fluency, semantic, and word generation. Our findings show that TLE is associated with bilateral alterations in both memory and language networks.

Altered functional connectivity in the memory network

In the encoding tasks, the number of significant directional connections with hyperconnectivity in TLE patients, compared with the control subjects, was higher than in retrieval tasks involving pictures and words. This indicates an extensive reorganization of the memory network in the encoding process and a degradation of the memory retrieval process in TLE patients.

Compared with the control subjects, in the picture encoding task, the hyperconnectivity in TLE patients mainly originated from the left areas expanding to both left and right regions (ipsilateral and contralateral). Notably, LHIP is one of the most effective sources of hyperconnectivity. This finding is consistent with previous studies reporting increased connectivity in the hippocampus in memory impairment,[21,34,35].

Despite an increase in connectivity observed in both left and right TLE groups compared with the control group, left TLE patients showed a remarkable decrease in connectivity from L-PHIP to R-EC compared with the RTLE group. This decrease suggests contralateral hypoconnectivity in left TLE patients compared to the RTLE.

Since the right side of the brain is more involved in visuospatial (nonverbal) memory,[24] our findings showed that memory reorganization in picture encoding is represented in the form of hyperconnectivity from the left side to the other areas.

In the picture retrieval task, the hyperconnectivity, especially in right TLE patients, originated from the LANG in the prefrontal cortex and extended from this region to the other areas. While other investigators have also reported the intervention of prefrontal areas in the memory network,[15,16,36,37] our results showed that this effect is initiated from the left hemispheric areas to the other intracranial regions. Also, our finding suggests an ipsilateral hypoconnectivity in PHIP. Namely, in left TLE patients, hypoconnectivity was seen from the L-PHIP to LP, whereas in right TLE patients, it was observed from the R-PHIP to LP. These results were also in agreement with the previous studies reporting the effect of PHIP on the memory retrieval process.[38–40] In particular, our work showed that directional connectivity from PHIP to L-P has decreased, indicating a reduced capacity of TLE patients in the memory retrieval process.

These results further indicate that PHIP hypoconnectivity was associated with the seizure foci. Comparison of left and right TLE patients also showed a bilateral hypoconnectivity in the HIP and PHIP areas. This hypoconnectivity, which was seen from the left to the right brain hemisphere in left TLE patients and occurred in the opposite direction in the right TLE patients, confirmed

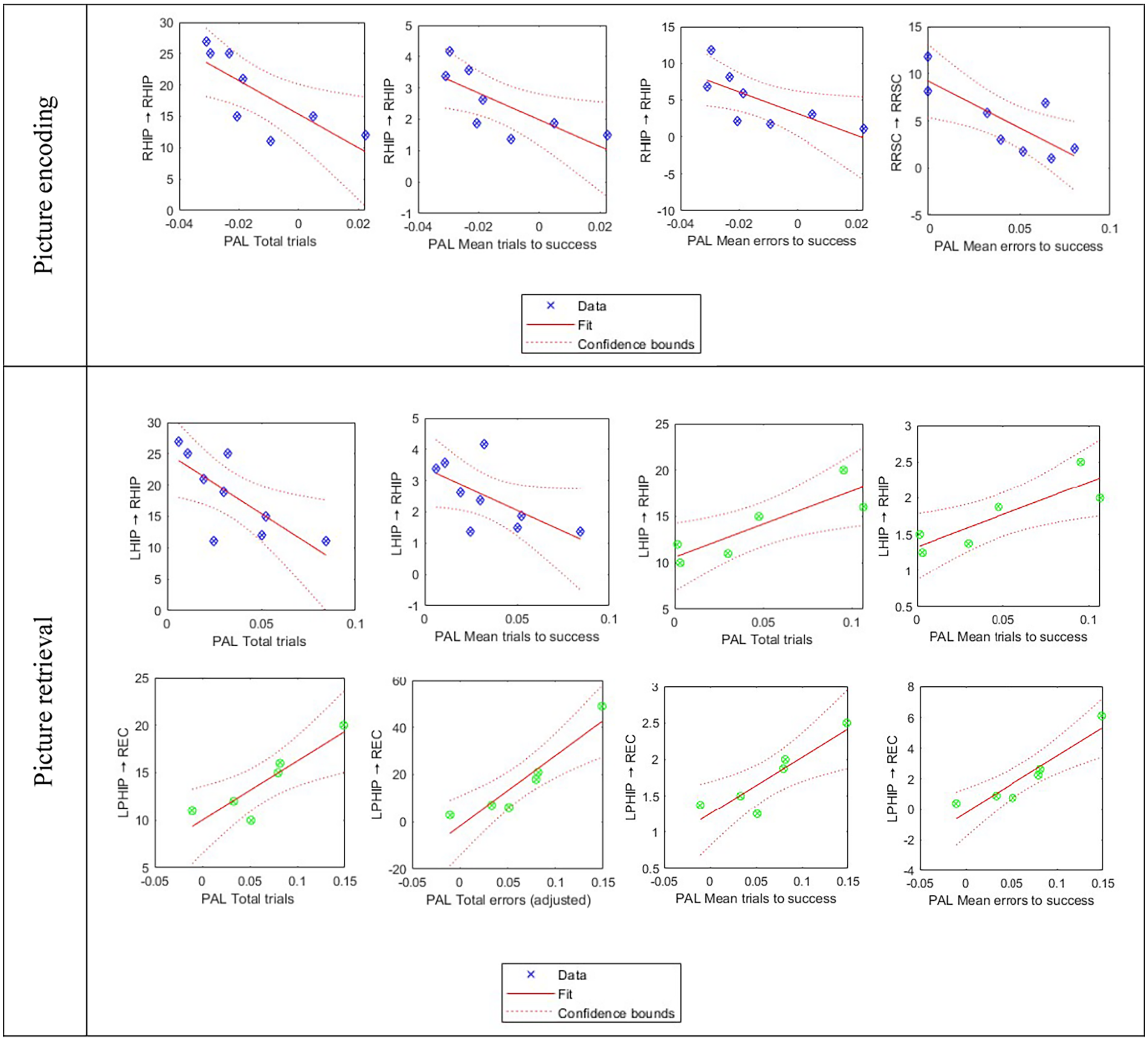

Figure 8. Correlation between significant connections between the left and right TLE groups and CANTAB PAL and PRM tests in picture encoding and retrieval tasks. Only correlations that have significant linear relations are represented. Blue colors and green colors are related to the left and right TLE groups, respectively. LHIP, left hippocampus; LPHIP, left parahippocampus; REC, right entorhinal cortex; RHIP, right hippocampus.

the role of HIP and P-HIP in the memory retrieval process. These connections may be therefore used as biomarkers for the lateralization of TLE patients.

In the word task, the significantly altered connections occurred more prominently in the right TLE group compared with the left TLE group. In the right TLE group, the hyperconnectivity was more pronounced in the right hemisphere. In the both right and left TLE groups, our findings showed hyperconnectivity extending from the LHIP to the other intracranial regions.

In verbal memory task, due to the participation of language areas, the left side of the brain was found to be more involved. Our findings showed that the memory reorganization in word encoding is represented in the form of hyperconnectivity from the right brain's hemisphere to the other intracranial areas.

In word retrieval, connectivity from the MPFC to L-RSC and R-RSC plays an essential role in the right TLE group. In comparing left and right TLE groups, the hyperconnectivity seen from the L-THA to L-PRC may be

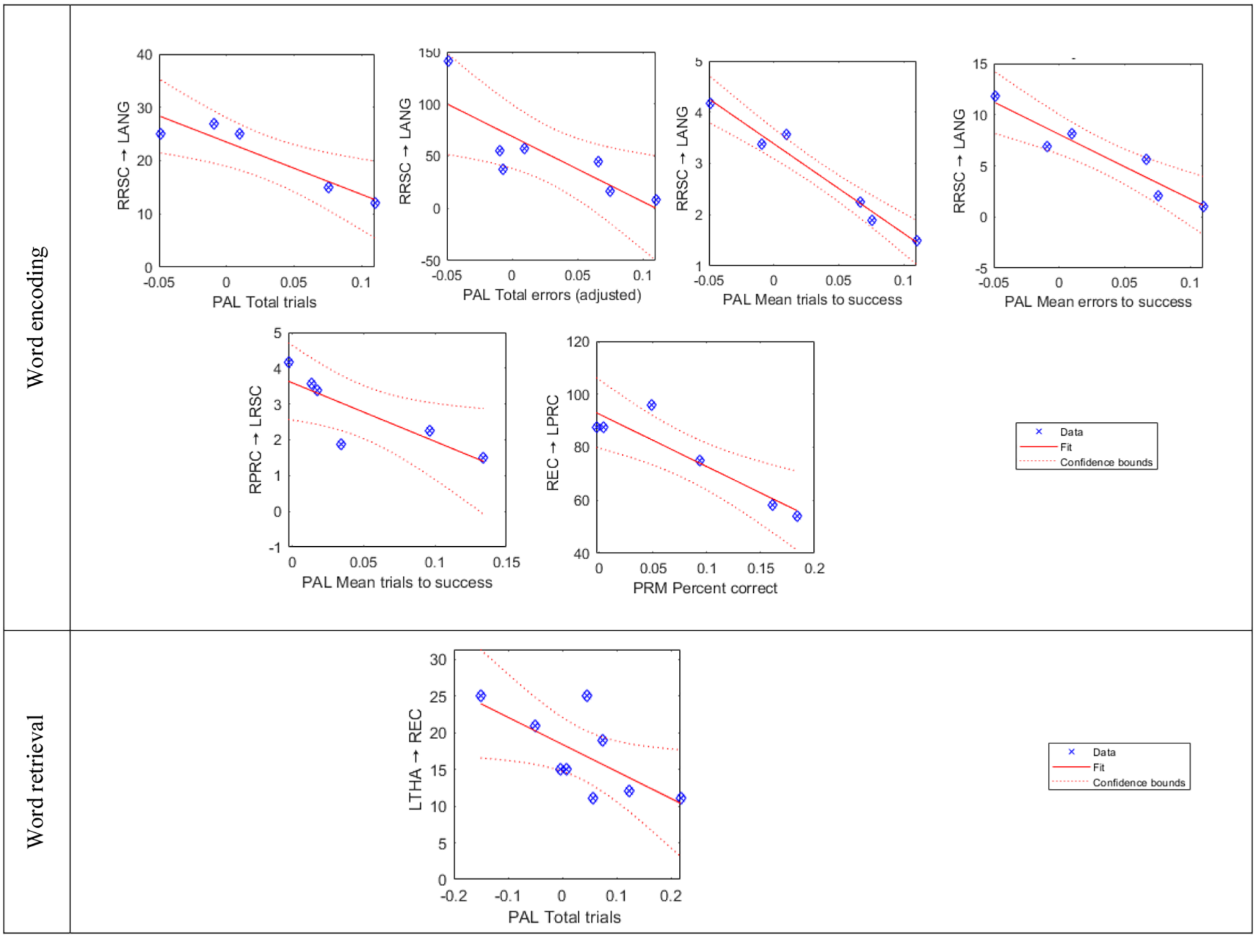

Figure 9. Correlation between significant connections between the left and right TLE groups and CANTAB PAL and PRM tests in word encoding and retrieval tasks. Only correlations that have significant linear relations are represented. Blue colors and green colors are related to the left and right TLE groups, respectively. LANG, Left angular; LPRC, left perirhinal cortex; LRSC, left retrosplenial cortex; LTHA, left thalamus; REC, right entorhinal cortex; RRSC, right retrosplenial cortex; RPRC, right perirhinal cortex.

potentially used as a biomarker for TLE lateralization. In the word encoding task, an increase in connectivity from L-THA to L-PRC was observed. On the contrary, comparing the left and right TLE groups concerning the picture task, the hypoconnectivity of the HIP and PHIP played a leading role, while in the word task, the hyperconnectivity of ANG and THA showed a dominant effect.

Altered functional connectivity in the language network

The nodes of the language network are primarily located in the left hemisphere, but several studies have shown the involvement of the right hemispheric areas in the language network, especially in cases of left TLE. Accordingly, we chose some nodes in the right hemisphere in DCM analysis. Our results based on DCM analysis indicate that the connections between the right and left hemispheres are significantly reduced. A hypoconnectivity was found between the right hemisphere and the Wernicke area, indicating the compromised and reduced influence of the right hemisphere over speech production in TLE patients.

In passive and semantic tasks, a comparison of the left and right TLE groups against the control group showed a decrease in connectivity, with the connections often formed from the left to the right areas.

In all passive, semantic, and verbal fluency tasks, the involvement of frontal areas was observed in the left TLE group. Performance of the passive tasks was associated with a decrease in the connectivity from Broca's area to the left temporal region, whereas for the verbal fluency tasks, there was increased communication between Broca's area and the frontal lobe regions. In all passive, semantic, and verbal fluency tasks, the right TLE group displayed a decrease in the connectivity between Wernicke's area and R-TP.

Relation of functional connectivity and psychological tests

About both the encoding and retrieval processes, a significant linear negative correlation was observed between the connectivity of the left TLE group and CANTAB test results, whereas a positive correlation was seen between the connectivity of the right TLE group and CANTAB test results. These significant correlations were associated with the PAL error and the PAL trial factors, where an increase in the corresponding scores indicates a decrease in memory performance.

This CANTAB score increase was related to reducing the directional connectivity in the left TLE group. The decrease in connectivity in the picture retrieval task was associated with the effect of LHIP on RHIP. This finding was in agreement with findings in previous sections of reduced hippocampal connectivity in picture retrieval. In addition, it showed that in LTLE patients, poor memory function leads to a decrease in hippocampal connections from the left to the right hemisphere. In the word encoding task, this decrease in connectivity was associated with the effective connection from the RPRC on the LANG, both of which are involved in word processing.

The positive correlation of PAL CANTAB scores and connectivity measures in the right TLE group, the increased connectivity was associated with an outperformance of the memory. This increase in connectivity in the picture retrieval task was associated with the effective connection from the LHIP to RHIP and from the LHIP to REC. These findings suggested a reorganization of memory in RTLE patients perturbed by increased interhemispheric connectivity.

Limitations and future works

One of the distinctions between our work and previous studies about the application of the DCM method is the examination of more regions within the memory and language networks in the DCM analysis. However, this approach limits the study of different models to determine the effects of tasks on different regions and connections based on the given model. Given the extensive number of regions and the myriad of potential connectivity, we chose to focus on the proposed model based on the entire connections in both memory and language networks. In our future studies, we intend to reduce the number of regions to compare several relevant models concerning different tasks.

Conclusion

Dynamic causal modeling of memory and language functional networks indicated the overt increase in brain connectivity detected by the encoding tasks and its relative decrease seen by the retrieval tasks reveals an interesting aspect of the performance of the memory network in TLE. Interestingly, the hyperconnectivity in encoding tasks was from the contralateral side of brain involvement in nonverbal (mostly right) and verbal (mostly left) memory. In the picture encoding task, this hyperconnectivity was mainly from the left side to the other regions, and in the word encoding task from the right side to the other regions. Hypoconnectivity in the retrieval tasks was from the contralateral side concerning TLE laterality. It is also noteworthy to emphasize the role of brain regions in the right hemisphere in the language network and the reduction of the connectivity between the brain hemispheres in TLE.

Author Contributions

All authors contributed to the study conception and design. Material preparation and data collection were performed by Mohammad-Reza Nazem-Zadeh, Fatemeh Eivazi, Neda Mohammadi Mobarakeh, and Hamed Dehghani-Siahaki1. Data analysis was performed by Alireza Fallahi. Patient selection and neurological findings were performed by Narges Hoseini-Tabatabaei, Jafar Mehvari Habibabadi, Seyed Sohrab Hashemi-Fesharaki, and Majid Barekatein. Psychological assessments were performed by Laila Alibiglou, Reza Rostami, and Mohammad Taghi Joghataei. Mohammad-Reza Nazem-Zadeh was the supervisor of this work. The first draft of the manuscript was written by Alireza Fallahi and all authors commented on the final versions of the manuscript.

Acknowledgement

The authors recognize the significant contribution of the Iranian National Brain Mapping Laboratory (NBML), Tehran, Iran, for data acquisition services. Also, the authors would like to acknowledge support from Iran Cognitive Sciences & Technologies Council.

Conflict of Interest

There is no conflict of interest for any of the authors to disclose.

Funding Information

This work was partially funded and supported by Cognitive Sciences & Technologies Council (Grant No. 6431), between 2017 and 2021.

Informed Consent

Informed consent was obtained from all individual participants included in the study.

Data Availability Statement

Data used in the preparation of this manuscript were obtained from project founded by Cognitive Sciences & Technologies Council (Grant No. 6431) and will be available upon request of authors.

References

1. Wiebe S, Blume WT, Girvin JP, Eliasziw M. A randomized, controlled trial of surgery for temporal-lobe epilepsy. N Engl J Med. 2001;345:311-318.
2. Berg AT, Scheffer IE. New concepts in classification of the epilepsies: entering the 21st century. Epilepsia. 2011;52:1058-1062.
3. Alessio A, Pereira FRS, Sercheli MS, et al. Brain plasticity for verbal and visual memories in patients with mesial temporal lobe epilepsy and hippocampal sclerosis: an fMRI study. Hum Brain Mapp. 2013;34:186-199.
4. Jaimes-Bautista AG, Rodríguez-Camacho M, Martínez-Juárez IE, Rodríguez-Agudelo Y. Semantic processing impairment in patients with temporal lobe epilepsy. Epilepsy Res Treat. 2015;2015:1-8.
5. Metternich B, Buschmann F, Wagner K, Schulze-Bonhage A, Kriston L. Verbal fluency in focal epilepsy: a systematic review and meta-analysis. Neuropsychol Rev. 2014;24:200-218.
6. Friston KJ. Functional and effective connectivity in neuroimaging: a synthesis. Hum Brain Mapp. 1994;2:56-78.
7. Baxendale S, Thompson PJ, Sander JW. Neuropsychological outcomes in epilepsy surgery patients with unilateral hippocampal sclerosis and good preoperative memory function. Epilepsia. 2013;54:e131-e134.
8. Jarčušková D, Palušná M, Gazda J, Feketeová E, Gdovinová Z. Which clinical and neuropsychological factors are responsible for cognitive impairment in patients with epilepsy? Int J Public Health. 2020;65:947-956.
9. Binder JR, Swanson SJ, Sabsevitz DS, Hammeke TA, Raghavan M, Mueller WM. A comparison of two fMRI methods for predicting verbal memory decline after left temporal lobectomy: language lateralization versus hippocampal activation asymmetry. Epilepsia. 2010;51:618-626.
10. Strandberg M, Mannfolk P, Stenberg L, et al. A functional MRI-based model for individual memory assessment in patients eligible for anterior temporal lobe resection. Open Neuroimag J. 2017;11:1-16.
11. You X, Zachery AN, Fanto EJ, et al. fMRI prediction of naming change after adult temporal lobe epilepsy surgery: activation matters. Epilepsia. 2019;60:527-538.
12. Friston KJ, Preller KH, Mathys C, et al. Dynamic causal modelling revisited. Neuroimage. 2019;199:730-744.
13. Friston KJ. Functional and effective connectivity: a review. Brain Connect. 2011;1:13-36.
14. Sidhu MK, Stretton J, Winston GP, et al. Memory network plasticity after temporal lobe resection: a longitudinal functional imaging study. Brain. 2016;139:415-430.
15. Campo P, Garrido MI, Moran RJ, et al. Network reconfiguration and working memory impairment in mesial temporal lobe epilepsy. Neuroimage. 2013;72:48-54.
16. Banjac S, Roger E, Cousin E, et al. Mapping of language-and-memory networks in patients with temporal lobe epilepsy by using the GE2REC protocol. Front Hum Neurosci. 2022;15:752138.
17. Jokeit H, Okujava M, Woermann FG. Carbamazepine reduces memory induced activation of mesial temporal lobe structures: a pharmacological fMRI-study. BMC Neurol. 2001;1:6.
18. Barrós-Loscertales A, Meseguer V, Sanjuán A, et al. Behavioral Inhibition System activity is associated with increased amygdala and hippocampal gray matter volume: a voxel-based morphometry study. Neuroimage. 2006;33:1011-1015.
19. Schacher M, Winkler R, Grunwald T, et al. Mesial temporal lobe epilepsy impairs advanced social cognition. Epilepsia. 2006;47:2141-2146.
20. Hamandi K, Powell HWR, Laufs H, et al. Combined EEG-fMRI and tractography to visualise propagation of epileptic activity. J Neurol Neurosurg Psychiatry. 2008;79:594-597.
21. Fleury M, Buck S, Binding LP, et al. Episodic memory network connectivity in temporal lobe epilepsy. Epilepsia. 2022;63:2597-2622. doi:10.1111/epi.17370
22. Dauvermann MR, Moorhead TWJ, Watson AR, et al. Verbal working memory and functional large-scale networks in schizophrenia. Psychiatry Res Neuroimaging. 2017;270:86-96.
23. Baddeley A. Working memory: theories, models, and controversies. Annu Rev Psychol. 2012;63:1-29.
24. Powell HWR, Richardson MP, Symms MR, et al. Reorganization of verbal and nonverbal memory in temporal lobe epilepsy due to unilateral hippocampal sclerosis. Epilepsia. 2007;48:1512-1525.

25. Wager TD, Smith EE. Neuroimaging studies of working memory. Cogn Affect Behav Neurosci. 2003;3:255-274.
26. Hertrich I, Dietrich S, Ackermann H. The margins of the language network in the brain. Front Commun. 2020;5.
27. Zhang Y, Wang K, Yue C, et al. The motor features of action verbs: fMRI evidence using picture naming. Brain Lang. 2018;179:22-32.
28. Pulvermüller F. Neural reuse of action perception circuits for language, concepts and communication. Prog Neurobiol. 2018;160:1-44.
29. Bookheimer S. Functional MRI of language: new approaches to understanding the cortical organization of semantic processing. Annu Rev Neurosci. 2002;25:151-188.
30. Sidhu MK, Stretton J, Winston GP, et al. A functional magnetic resonance imaging study mapping the episodic memory encoding network in temporal lobe epilepsy. Brain. 2013;136:1868-1888.
31. Kiran S, Meier EL, Kapse KJ, Glynn PA. Changes in task-based effective connectivity in language networks following rehabilitation in post-stroke patients with aphasia. Front Hum Neurosci. 2015;9:316.
32. Chai LR, Mattar MG, Blank IA, Fedorenko E, Bassett DS. Functional network dynamics of the language system. Cereb Cortex. 2016;26:4148-4159.
33. Benjamini Y, Hochberg Y. Controlling the false discovery rate: a practical and powerful approach to multiple testing. J R Stat Soc Ser B. 1995;57:289-300.
34. Jung A, Park C, seo Choi Y, Yoo JH, Lee HW. Functional brain connectivity and memory impairment in temporal lobe epilepsy (I7.007). Neurology. 2016;86: I7.007.
35. Ren Y, Nguyen VT, Sonkusare S, et al. Effective connectivity of the anterior hippocampus predicts recollection confidence during natural memory retrieval. Nat Commun. 2018;9:4875.
36. Qin L, Jiang W, Zheng J, Zhou X, Zhang Z, Liu J. Alterations functional connectivity in temporal lobe epilepsy and their relationships with cognitive function: a longitudinal resting-state fMRI study. Front Neurol. 2020;11:1-10.
37. Hill PF, King DR, Lega BC, Rugg MD. Comparison of fMRI correlates of successful episodic memory encoding in temporal lobe epilepsy patients and healthy controls. Neuroimage. 2020;207:116397.
38. Dupont S. Episodic memory in left temporal lobe epilepsy: a functional MRI study. Brain. 2000;123:1722-1732.
39. Li, M., Lu, S., Li, J. & Zhong, N. The role of the parahippocampal cortex in memory encoding and retrieval. An fMRI Study. 2010:377–386. 10.1007/978-3-642-15314-3_36.
40. Daselaar SM, Rombouts SARB, Veltman DJ, Raaijmakers JGW, Lazeron RHC, Jonker C. Parahippocampal activation during successful recognition of words: a self-paced event-related fMRI Study. Neuroimage. 2001;13:1113-1120.

Supporting Information

Additional supporting information may be found online in the Supporting Information section at the end of the article.

Table S1. Significant hypo- and hyper connections in memory tasks and ones that survived FDR and ones that did not survive. *Survived FDR correction. (Effect size).
Table S2. Significant hypo- and hyper connections in language tasks and ones that survived FDR and ones that did not survive. *Survived FDR correction. (Effect size).

